

Understanding the Cognitive Process of the Human Visual System by Analysing Illusions Generated Using A Visual Characteristics Tester

Laiyou Huang*

School of Electronic Science and Engineering,
Nanjing University, China

*Corresponding Author

Laiyou Huang, School of Electronic Science and Engineering, Nanjing University, China.

Submitted: 2025, Nov 10; Accepted: 2025, Dec 08; Published: 2025, Dec 12

Citation: Huang, L. (2025). Understanding the Cognitive Process of the Human Visual System by Analysing Illusions Generated Using A Visual Characteristics Tester. *Int J Psychiatry*, 10(4), 01-10.

Abstract

Despite advances in vision research, how people see objects remains unclear. In this study, a WT5518 Visual Characteristics Tester imitating an electric fan was developed and used to investigate visual cognition. The tester could induce various visual illusions. Analysis of these visual illusions revealed that the human visual system consists of the high- and low-speed visual subsystems, in which the visual brain processes visual information from the high- and low-speed visual pathways, and consciousness recognizes visual information from the visual brain. The two subsystems are independent of each other and do not interfere with each other; however, at some speeds, there is an intersection between the two subsystems. Furthermore, human vision comprises two states, i.e. the visual “filming state,” and “staring state.” During the “filming state,” consciousness captures and recognizes images from the high- and low-speed visual brain simultaneously, so, at this moment the individual can see the surrounding scenes. During the “staring state,” consciousness does not capture any images, thus, at this moment the individual cannot see the surrounding scenes. Ultimately, visual information is discrete and intermittent. In the “staring state,” vision stares at the images taken previously, therefore, the intermittence of visual information can hardly be perceived. Alternation of the two visual states endows human vision with frequency characteristics. The frequency at which consciousness samples visual information is 100 Hz. The cognitive behavior of people’s vision is synchronous. Both high- and low-speed vision subsystems can create illusions but only high-speed vision can create afterimages. This study provides a foundation for cognitive research.

Keywords: Psychology, Neuroscience, Brain, Vision, Consciousness, Cognition

1. Introduction

Human vision involves the eyes, visual pathway system and the visual brain. The visual pathway system comprises three separate, independent visual paths, which process and transmit different aspects of the same retinal image to the corresponding brain regions [1,2]. The magnocellular pathway starts from rod photoreceptors and projects to M-cell layers, which consists of large axons in the lateral geniculate nucleus. The parvocellular pathway starts from cone photoreceptors and projects to P-cell layers, which consists of medium-sized axons in the lateral geniculate nucleus [3-5]. The koniocellular pathway starts from bistratified retinal ganglion

cells and projects to K-cell layers, which consists of small axons in the lateral geniculate nucleus [6,7]. The parvocellular and magnocellular pathways are selective for form/color and depth/movement of an object, respectively. Color, form, and motion are perceived at different times, with color being perceived first [8-10]. Human vision is associated with a perceptual temporal hierarchy [11-13]. The visual brain subsequently combines relevant visual attributes that are perceived asynchronously, generating a unified experience of the visual world [1,2,12].

Partial damage to the visual system of brain may result in partial loss of visual function, which suggests that brain recognizes visual information [14-16].

There are many scientists who believe that consciousness plays an important role in visual cognition, however, how consciousness recognizes visual information is not well explained [17,18].

Through the analysis of visual illusions, this study found the general rule of conscious recognition of visual information.

2. Materials and Methods

2.1. Ethics Statement

The study protocol was approved by the Medical Ethics Subcommittee of the Science and Technology Ethics Committee of Nanjing University (OAP20230829001). Written informed consents were obtained from all participants. All experiments were performed in accordance with relevant guidelines and regulations.

2.2. Participants and Experimental Equipment

A total of 72 volunteers (aged, 20–70 years; 36 men and 36 women excluding pregnant women) participated in the study and were randomly selected. The participants were divided into eight groups of nine participants each. At the end of each test, at least one of the participants participated in the next test. The participants stood or sat anywhere from 1 to 6 meters in front of the tester. To study the visual cognition, the WT5518 Visual Characteristics Tester was developed. The tester was composed of a motor, with a flange mounted on its axis, with several blades of different shapes. The rotational speed of the motor was manipulated using remote controls. The default rotation direction was clockwise. The tester could be used to induce various visual illusions by changing the number and shape of the blades on the flange and adjusting the rotational speed of the motor during the experiments.

3. Experiments

• Experiment 1: Visual Phenomena Induced by Rotating Blades

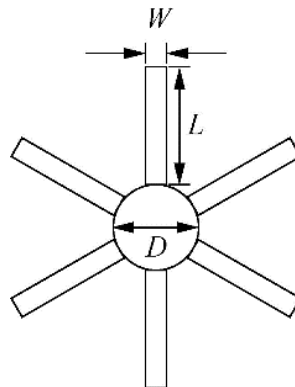


Figure 1: Diagram of the Group of Experimental Blades

The flange diameter (D) and the blade length (L) and width (W) were changeable. The number of the blades could be varied.

12 white identical rectangular blades were installed on the WT5518 Visual Characteristics Tester at 30° to each other. The flange diameter (D) was 8 cm, the blade length (L) was 11.3 cm and width (W) was 1.3 cm, as shown in (Figure. 1).

As the rotational speed of the motor was changed, a series of strange visual phenomena appeared.

(1) When the motor rotated between 0 and 62.5 rpm, all participants saw 12 white identical rectangular blades spaced at 30° rotating in a clockwise direction. The faster the speed, the more blurred the blades. When the motor rotated at 62.5 rpm, the outer parts of the blades were more blurred than the inner parts of the blades.

(2) When the motor rotated at 125 rpm, the inner parts of the 12 white identical rectangular blades could still be seen rotating clockwise. Simultaneously, all participants saw 48 identical fan-shaped blades spaced at 7.5° without rotation, but the inner parts

of the 48 fan-shaped blades disappeared and the inner parts of the 12 white rectangular blades always overlapped with the outer parts of one group of 12 fan-shaped blades.

(3) When the motor speed was set to 500 rpm, there may be a little deviation between the actual speed and the set speed. When the actual speed of the motor was equal to the set speed, 500 rpm, all participants saw the 12 fan-shaped blades fixed without rotation and the same 12 angles, as shown in Video 1.

When the actual speed of the motor was slightly higher than 500 rpm, all participants saw the 12 fan-shaped blades rotating slowly in a clockwise direction, as shown in Video 2.

When the actual speed of the motor was slightly below 500 rpm, all participants saw the 12 fan-shaped blades rotating slowly in an anticlockwise direction, as shown in Video 3.

Since the motor cannot always achieve the actual speed equal to the set speed, the participants saw that the blades sometimes

did not turn, sometimes slowly turned clockwise, and sometimes slowly turned counterclockwise.

In the above three cases, the 12 rectangular white blades disappeared completely from sight.

No matter how the blades turned, the participants saw the same result.

(4) When the motor rotated at 501 rpm, all participants saw 12 fan-shaped blades rotating slowly in a clockwise direction, as shown in Video 2.

(5) When the motor rotated at 499 rpm, all participants saw 12 fan-shaped blades rotating slowly in an anticlockwise direction, as shown in Video 3.

- **Experiment 2: Visual Afterimages Induced by High-Speed Rotating Blades**

A white rectangular blade was installed on the flange and a black rectangular blade with the same shape and mass was installed at an angle of 180° to the white blade as a counterweight. The flange diameter (D) was 8 cm, the blade length (L) was 11.3 cm and width (W) was 3.0 cm (Figure. 1). At high rotational speeds, only the white blade could be seen whereas the black blade was hidden by the black background. When the motor rotated at 750 rpm, all participants saw 8 fan-shaped blades at 45° between the blades without rotation. All participants produced visual afterimages.

- **Experiment 3: Visual Illusions Induced by High-Speed Rotating Blades**

Six white rectangular blades were installed at a 60° to each other. The flange diameter (D) was 8 cm, the blade length (L) was 11.3 cm and width (W) was 2.0 cm (Figure. 1). The motor was rotated clockwise at 1,000, 500, 333.3, 250, 200, 166.7, 142.9 and 125 rpm, all participants saw 6, 12, 18, 24, 30, 36, 42 and 48 fan-shaped blades at 60°, 30°, 20°, 15°, 12°, 10°, 8.6° and 7.5°, respectively, without rotation.

- **Experiment 4: Investigation of Synchronized Cognitive Behavior of Low- And High-Speed Vision**

48 white rectangular blades were installed at 7.5° to each other. The flange diameter (D) was 8 cm, the blade length (L) was 11.3 cm and width (W) was 0.4 cm (Figure. 1). When the motor was rotated clockwise at 125 rpm, all participants saw 48 white rectangular blades and 48 fan-shaped blades simultaneously, and they completely overlapped and fixed at 48 different angles without rotation, as shown in Video 4.

- **Experiment 5: Visual Illusions Produced by Low-Speed Rotating Blades**

100 white rectangular blades were installed at 3.6° to each other. The flange diameter (D) was 13 cm, the blade length (L) was 8.8

cm and width (W) was 0.4 cm (Figure. 1).

(1) When the motor rotated at 60 rpm, all participants saw 100 white rectangular blades fixed at 100 different angles without rotation, as shown in Video 5.

(2) When the motor rotated at 62 rpm, all participants saw 100 white rectangular blades rotating slowly in a clockwise direction.

(3) When the motor rotated at 58 rpm, all participants saw 100 white rectangular blades rotating slowly in an anticlockwise direction.

All the videos in this article were shot at a frequency of 30 fps at 60 cm in front of the tester. Some video-induced images were the same as those induced by the tester and used as demonstrations, while others were different from those induced by the tester and cannot be used as demonstration.

4. Results and Discussion

4.1. Visual System

Human Visual System Consists of High- And Low-Speed Vision and Consciousness Recognizes Visual Information In Experiment 1 (1), 12 white rectangular blades were rotated between 0 and 62.5 rpm, and all participants saw the 12 white rectangular blades spaced at 30° rotating in a clockwise direction. The visual system involved in seeing the 12 white rectangular blades was low-speed vision.

In Experiment 1 (3), 12 white rectangular blades were rotated at 500 rpm, and all participants saw 12 fan-shaped blades fixed at 12 angles of 30° without rotation (Video 1). The visual system involved in seeing the 12 fan-shaped blades was high-speed vision. In Experiment 1 (2), 12 white rectangular blades were rotated at a medium speed and the 12 white rectangular blades could still be seen rotating clockwise; however, all participants additionally saw 48 fan-shaped blades spaced at 7.5° without rotation. The shapes of the 12 white rectangular blades were identical to the 12 white rectangular blades in Experiment 1 (1), and therefore involved low-speed vision. The shapes of the 48 fan-shaped blades were similar to that in Experiment 1 (3), it's area was one quarter of that in Experiment 1 (3), and the number was four times of that in Experiment 1 (3), and therefore involved high-speed vision. As all participants saw both low- and high-speed visual information simultaneously, it can be inferred that human vision consists of low-speed (visualization of white rectangular blades at rest or rotating at low speed) and high-speed (visualization of fan-shaped blades rotating at high speed) vision.

Based on the above analysis and the results of vision research, this study draws the following conclusions:

The eyes, parvocellular system 1, 2, and one part of brain constitute a high-speed visual sensor. The parvocellular system is composed of medium-sized cells, which are sensitive only to information related to high-speed motion. The high-speed visual sensor forms a high-speed vision with consciousness (Figure. 2).

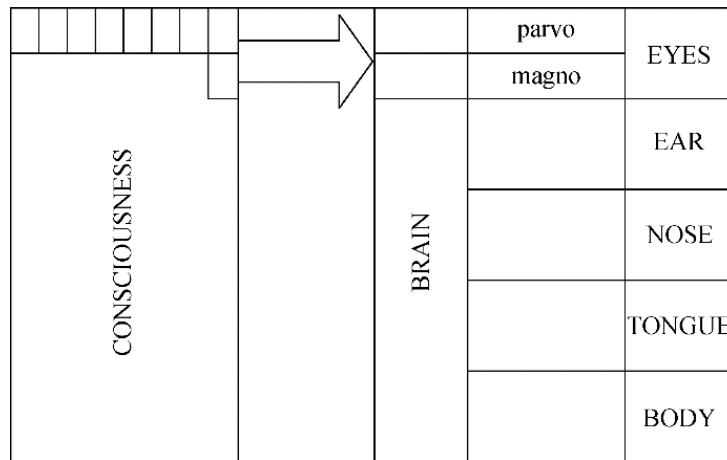


Figure 2: Searching Diagram of Consciousness

Consciousness constantly searches the parts of the brain associated with the eyes, ears, nose, tongue and body, and identifies the information.

The eyes, magnocellular system and another part of brain constitute a low-speed visual sensor [1,2]. The magnocellular system is composed of large cells, which are sensitive only to information related to rest and low-speed motion. The low-speed visual sensor forms a low-speed vision with consciousness (Figure. 2).

The Experiment 1 (2) also demonstrated that high- and low-speed vision were independent of each other and did not interfere with each other, and at some speeds, there was an intersection between them.

The eyes convert light information into a bioelectrical signal, and the high- and low-speed information in the bioelectrical signal is transmitted to the visual brain via high- and low-speed visual pathways, respectively. The visual brain processes the two separate streams of information; however, the visual information is unrecognizable. Consciousness is required to sample the high- and low-speed visual information and produce cognition separately by comparing the incoming information with known information, thereby allowing sight [20,21]. Visual cognition is therefore not possible without consciousness (Figure. 2) [13,19].

It is also supported by clinical evidence that vision consists of two visual subsystems. There is a kind of movement blindness (caused by damage to the V5 area of the cerebral cortex). They can see stationary object, but not moving object. Others suffer from imperceptible forms (often accompanied by color blindness, in which only gray shadows are seen). These patients have great difficulty recognizing object when they are at rest, but have little or no difficulty seeing them when they are moving.

Several observations support the conclusion that consciousness is required to recognize visual information.

First, visual information is continuously transmitted from the eyes to the visual brain; however, the visual information is not continuous, suggesting that the destination of visual information is not the visual brain, but consciousness.

Second, visual information regarding various aspects of an object, such as color, shape, and motion, is transmitted to the visual brain at different times and the visual brain cannot assimilate these asynchronous features. Instead, consciousness samples visual information from the visual brain, combines relevant visual attributes by comparing incoming information with previous knowledge, and provides a unified visual world [13,22].

Third, partial damage to the visual brain, resulting in partial loss of visual function, cannot be proven to be caused by the loss of cognitive function of the visual brain. As partial damage to the visual brain tissues results in the loss of the visual brain's ability to process information, consciousness does not have access to relevant visual information, resulting in partial loss of visual function.

Deep sleep is an example of a situation in which only consciousness, not brain, can recognize information. When a person is awake, consciousness constantly searches the auditory brain and recognizes sound information so that the person can hear it. During deep sleep, consciousness does not search the auditory brain and the person can therefore not hear the sounds.

5. High-Speed Vision

5.1. High-Speed Visual Information Is Discrete and Intermittent

In Experiment 1(3), despite continuous rotation, the participants did not observe rotation, which suggests that high-speed vision functions similar to a movie camera, alternating between registering pieces of high-speed visual information and pausing. When the shooting frequency of the high-speed vision synchronizes with the rotational frequency of the motor, the blades are seen as fixed at certain angles, without rotation (Video 1).

Based on the above analysis, the working mechanism of high-speed vision is as follows:

When consciousness examines the high-speed visual brain, vision is in the “filming state,” and consciousness captures one image from the high-speed visual brain. Consciousness subsequently recognizes the image and generates new cognition by comparing incoming information with previous knowledge. Only then are the image seen. When consciousness leaves the high-speed visual brain, vision is in the “staring state,” during which consciousness does not capture any image and scenes cannot be seen. Consciousness continuously alternates between the “filming” and “staring” states, and ultimately, high-speed visual information becomes discrete and intermittent. In the “staring state,” the high-speed vision stares at the information taken previously, therefore, the intermittence of high-speed visual information can hardly be perceived.

5.2. High-Speed Visual Frequency F_h

The alternation between the two visual states endows high-speed vision with frequency characteristics. In Experiment 1 (3), when the actual rotating speed of the motor was 500 rpm, all participants saw 12 fan-shaped blades fixed at 12 angles of 30° without rotation. High-speed vision captured an image when the motor rotated by 30° , so, during one rotational cycle, 12 images were captured by high-speed vision, and 12 frequency synchronizations between the shooting frequency of high-speed vision and the rotational frequency of the motor occurred (Video 1).

High-speed visual frequency can be calculated as equation (1) and (2), with n representing the rotational speed of the motor, f representing the rotational frequency of the motor, f_h representing the shooting frequency of high-speed vision, and T_h representing the filming period of high-speed vision.

Then, in Experiment 1 (3):

$$f = \frac{n}{60} = \frac{500}{60} \approx 8.33 \text{ (Hz)} \quad (1)$$

$$f_h = f \times 12 = 8.33 \times 12 \approx 100.0 \text{ (Hz)} \quad (2)$$

$$T_h = \frac{1}{f_h} = \frac{1}{100} = 10 \text{ (ms)} \quad (3)$$

Numerous studies have shown that $f_h = 100$ Hz is the only operating frequency for high-speed vision.

A photoelectric sensor composed of infrared transmitting and receiving tubes was mounted on the base plate of the tester. The photoelectric sensor emits a pulse each time a rotating blade passes through it. During each rotational cycle of the motor, the 12 blades pass through the photoelectric sensor successively and the photoelectric sensor emits 12 pulses in total. The total number of pulses emitted by the photoelectric sensor in 1 s is equal to the shooting frequency of the high-speed vision system.

A 18F45K80 microchip was used as the main control chip for WT5518 visual characteristics tester. The photoelectric sensor output was connected to the T1CKI input end of the 18F45K80 microchip timer1, and timer1 was set as the counter. Timer0 was set to a timer interval of ten seconds. After receiving the interruption, 18F45K80 reads out the data in timer1 and divides it by 10. The number of blades passing through the photoelectric sensor in 1 s, namely, the shooting frequency of the high-speed vision was found to be 99.8–100.2 Hz.

The photoelectric sensor output pulse was measured using a UNI-T Digital Storage Oscilloscope (UTD2102CEX), and found to be the result 99.2–100.5 Hz.

The frequency tested using 18F45K80 was the average frequency within ten seconds, and the fluctuation range was therefore relatively small. In contrast, the immediate frequency was measured using the oscilloscope, and the fluctuation range was therefore relatively large.

Although the two test methods were different and the fluctuation ranges were not the same, the calculated high-speed visual frequency, f_h , was always between the values obtained using the two measurement methods, suggesting that high-speed visual frequency f_h can be calculated using the motor speed.

5.3. The Cognition Behavior of People’s High-Speed Vision Is Synchronous

In Experiment 1 (3), the participants saw 12 fan-shaped blades fixed at 12 different angles. The 12 angles visualized were the same for all participants, which indicated that all participants’ high-speed vision was in the “filming state” and the “staring state” at the same time, which suggested that the cognitive behavior of all participants’ high-speed vision was synchronous, implying that people’s high-speed visual cognitive behavior is synchronous, as shown in the Video 1. Experiment 1 (3), (4) and (5) showed that if a person’s visual frequency had a difference of $1/600$, he would see the blades rotating slowly clockwise as in Experiment 1 (4) or anticlockwise as in Experiment 1 (5), while others see the blades not rotating when the motor rotated at 600 rpm.

Therefore, there must be one “common visual clock” outside human body to time consciousness. Based on the frequency characteristics of human vision, this study concluded that the “common visual clock” may be one pulsar with a rotational frequency of 50 Hz, sent out as two pulses in one rotation. Similar to “quantum entanglement”, there is an “entanglement effect” between vision and the pulses emitted by the pulsar. The pulses induce people’s vision to enter the “filming state” and consciousness simultaneously captures image from the visual brain.

5.4. Temporary Storage Buffer of High-Speed Visual Information

In Experiment 2, the relationship between the rotating speed, n_k , and the number of visualised fan-shaped blades, k , and the rotating frequency, f_k , can be expressed as follows:

$$n_k = \frac{fh \times 60}{k} \quad (4)$$

$$= \frac{6000}{k} \text{ (rpm)} \quad (k=1, 2, 3 \dots)$$

For example, when $k = 8$, the rotating speed of the motor is $n_8 = 6000/8 = 750$ rpm. At a rotational speed of 750 rpm, all the participants saw eight fan-shaped blades, with 45° between the blades, without rotation.

Experiment 2 therefore demonstrates a “first-in, first-out” temporary storage buffer of high-speed visual information in high-speed vision. High-speed vision constantly extracts information from the high-speed visual brain and temporarily stores the discrete stream of the high-speed visual images into the temporary storage buffer of high-speed visual information. The rotational frequency of the motor is $f_8 = n_8 / 60 = 12.5$ Hz, and high-speed vision obtained eight images during one rotational cycle because the shooting frequency of high-speed vision $f_h = 100$ Hz was eight times f_8 . Owing to the different shooting times, the blades in adjacent images were positioned 45° to each other, and participants saw eight fan-shaped blades at an angle of 45° between the blades, without rotation, as a result of the superposition of the eight discrete images in the temporary storage buffer of high-speed visual information. Such superposition of discrete information led to visual afterimages.

The WT5518 Visual Characteristics Tester indicated that the temporary storage buffer of high-speed visual information can save at least eight images simultaneously. Further research is required to investigate whether this temporary storage buffer has a greater storage capacity.

In Experiment 3, the high-speed visual illusions can be described as follows:

$$n_{i \times k} = \frac{fh \times 60}{i \times k} \quad (5)$$

$$= \frac{6000}{i \times k} \text{ (rpm)} \quad (i \times k \leq 120)$$

where i represents the number of installed blades, k is a natural number, and $n_{i \times k}$ represents the rotational speed of the motor. When the motor rotated at $n_{i \times k}$, all the participants saw $i \times k$ fan-shaped blades, without rotation. This illusion is caused by the same principles described for Experiment 2. If $i = 1$, equation (5)

yields equation (4); therefore, equation (5) represents the general expression for these visual illusions.

If $i = 12$ and $k = 1$, then $n_{i \times k} = n_{12} = 6000/12 = 500$ rpm. When the motor rotates at 500 rpm, all participants see 12 fan-shaped blades with 30° between the blades without rotation, which is the equivalent of Experiment 1 (3). As the 12 blades are the same, the image composed of the 12 blades is the same as the image after rotating through 30° . The shooting frequency of high-speed vision is 12 times the rotational frequency of the motor, so, high-speed vision captures 12 images in total during one rotational cycle, that is, high-speed vision captures an image every 30° of rotation of the blades, and sequentially stores the captured images into the temporary storage buffer of high-speed visual information. Assume that the storage capacity of the temporary storage buffer of high-speed visual information is 8. The 8 images in the temporary storage buffer of high-speed visual information are the same, and superposition of eight identical images therefore allows participants to see the 12 fan-shaped blades fixed at certain angles without rotation.

If $i = 12$ and $k = 4$, then $n_{i \times k} = n_{48} = 6000/48 = 125$ rpm. When the motor rotates at 125 rpm, all participants see 48 fan-shaped blades with 7.5° between the blades without rotation, which is the equivalent of Experiment 1 (2). The shooting frequency of high-speed vision is 48 times the rotational frequency of the motor, so, high-speed vision captures 48 images in total during one rotational cycle, that is, high-speed vision captures an image every 7.5° of rotation of the blades, and sequentially stores the captured images into the temporary storage buffer of high-speed visual information, thus, images 1 and 5; 2 and 6; 3 and 7; and 4 and 8 are the same, and superposition of the eight images in the temporary storage buffer of high-speed visual information allows all participants to see the 48 fan-shaped blades fixed at certain angles without rotation.

Investigation of the visual illusion of clockwise rotation induced by high-speed rotating blades In equation (5), when the motor rotates clockwise at a speed of $n_{i \times k} + \Delta n_{i \times k}$ rpm, all observers see blades rotating slowly in a clockwise direction. For example, if $i = 12$ and $k = 1$, then $n_{12 \times 1} + 1 = 501$ rpm. When the motor rotates clockwise at 501 rpm, all observers see blades rotating slowly in a clockwise direction as shown in Experiment 1 (4) (Video 2). The visual illusion of clockwise rotation can be explained by a single-blade experimental system (Figure. 3).

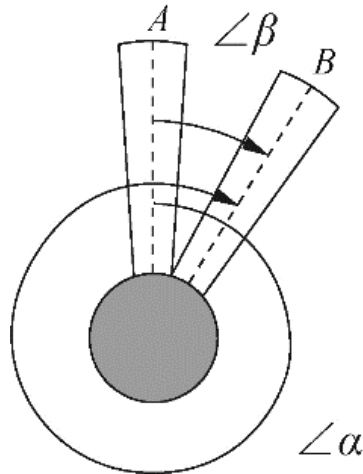


Figure 3: Diagram of the Visual Illusion of the Clockwise Rotation

The blade rotates at a high speed in a clockwise direction, while all observers see the blade rotates slowly in a clockwise direction.

When high-speed vision is in the “filming state,” all observers see the blade in position A. This is followed by the “staring state.” During the “staring state,” all observers only stare at the captured information and do not see the rotating blades in front of them. The “filming state” appears again, and owing to the acceleration of the rotational speed, the blade has moved from position A to position B. Because $\angle\alpha > \angle\beta$, (on the principle of “smallness” of Gestalt theory), all observers see the two blades with the included $\angle\beta$ as an interrelated whole, therefore, the perception is that the blade

rotates at $\angle\beta$, from A to B, slowly in the clockwise direction.

5.5. Investigation of the Visual Illusion of Anticlockwise Rotation Induced by High-Speed Rotating Blades

In equation (5), when the motor rotates clockwise at a speed of $n_{i \times k} - \Delta n_{i \times k}$ rpm, all observers see blades rotating slowly in an anticlockwise direction. For example, if $i = 12$ and $k = 1$, then $n_{12 \times 1} - 1 = 499$ rpm. When the motor rotates clockwise at 499 rpm, all observers see blades rotating slowly in an anticlockwise direction as shown in Experiment 1 (5) (Video 3). The visual illusion of anticlockwise rotation can be explained by a single-blade experimental system (Figure. 4).

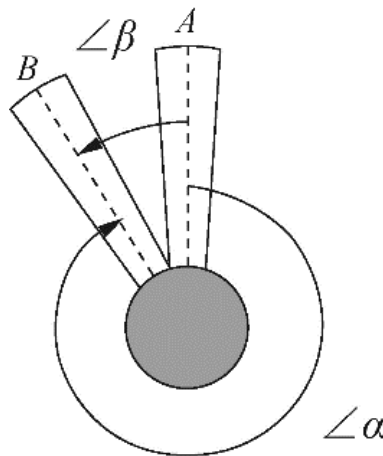


Figure 4: Diagram of the Visual Illusion of the Anticlockwise Rotation

The blade rotates at a high speed in a clockwise direction, while all observers see the blade rotates slowly in an anticlockwise direction.

When the high-speed vision is in the “filming state,” all observers see the blade in position A. This is followed by the “staring state.” During the “staring state,” all observers only stare at the captured

information and do not see the rotating blades in front of them. The “filming state” appears again, and owing to the decrease in rotational speed, the blade only reaches position B instead of position A. Because $\alpha > \beta$, and all observers see the two blades with the included β as an interrelated whole, yielding a perception that the blade rotates at β , from A to B, slowly in an anticlockwise direction.

6. Characteristics of High-Speed Vision

When high-speed vision captures images from the high-speed visual brain, the blades rotate at high speed. The image is therefore perceived as a fan-shaped area formed by the rotation of the blades during the “filming state” duration.

The parvocellular system in high-speed vision is similar to a high-pass filter; it transmits only high-speed motion information within a certain range to the high-speed visual brain, preventing transmission of information regarding blades rotating at low speed. When the rotational speed was decreased to 125 rpm, the inner parts of the 48 fan-shaped blades were blocked first by the parvocellular system and began to disappear from high-speed vision because the linear speed of the inner parts of the blades was slower than that of the outer parts of the blades. When the rotational speed was decrease to 62.5 rpm, the fan-shaped blades completely disappeared from high-speed vision.

7. Low-Speed Vision

7.1. Cognitive Behavior of Low- and High-Speed Vision is Synchronized

Experiment 4 indicated that the cognitive behavior of low- and high-speed vision was synchronized and implied that low-speed visual information was also discrete and intermittent (Video 4). As the working frequency of low-speed vision is also 100 Hz, this frequency can be referred to as human visual frequency. The cognitive behavior of the participants’ low-speed vision is also synchronous.

7.2. Temporary Storage Buffer of Low-Speed Visual Information

Low-speed visual information is discrete and intermittent, but the intermittence can hardly be perceived. This indicates that there is a temporary storage buffer of low-speed visual information. Experiments 4 and 1 (2) used the same rotational speed of 125 rpm. In Experiment 4, 48 white rectangular blades were installed and participants saw 48 white rectangular blades. In Experiment 1 (2), 12 white rectangular blades were installed, and participants saw 12 white rectangular blades without visual afterimage. This indicates that the temporary storage buffer of low-speed visual information could only store one piece of visual information.

7.3. Investigation of illusions induced by low-speed rotating blades

Experiment 4 and Experiment 5 (1) indicated that when the motor speed and number of blades meet the criteria defined in equation (6), all the participants saw m white rectangular blades without rotation (Video 5).

$$n_m = \frac{6000}{m} \text{ (rpm)} \quad (48 \leq m) \quad (6)$$

Equation (6) is similar to equations (4) and (5); however, the k and $i \times k$ in equation (4) and (5) include visual afterimages, whereas the m in equation (6) only represents the actual number of blades. In addition, m must be greater than or equal to 48.

Experiment 5 (1), (2) and (3) showed that low-speed vision can produce illusions just like high-speed vision.

7.4. Characteristics of Low-Speed Vision

Low-speed vision allows the perception of color, form, position, and depth of an object at rest or moving at low speed.

The magnocellular system in low-speed vision is similar to a low-pass filter, transmitting information about resting conditions or slow motion to the low-speed visual brain, which prevents transmission of information regarding fast motion. At rotational speeds between 0 and 62.5 rpm, 12 white rectangular blades were visible; at 62.5 rpm, the outer parts of the blades blurred more than the inner parts of the blades because the linear speed of the outer parts of the blades was greater than that of the inner parts of the blades. At a rotational speed of 500 rpm, the 12 white rectangular blades completely disappeared.

8. Conclusion

The human visual system consists of the high- and low-speed visual subsystems, in which the visual brain processes visual information from the high- and low-speed visual pathways, and consciousness recognizes visual information from the visual brain. The two subsystems are independent of each other and do not interfere with each other; however, at some speeds, there is an intersection between the two subsystems. Consciousness samples the high- and low-speed visual brain simultaneously at a frequency of 100 Hz. When consciousness captures images from the high- and low-speed visual brain, an individual is in the visual “filming state,” during which they can see the surrounding scenes. When consciousness leaves the visual brain, an individual is in the visual “staring state,” during which he cannot see the surrounding scenes. Ultimately, visual information is discrete and intermittent, and visual cognitive behavior is synchronous. Both high- and low-speed vision can create illusions but only high-speed vision can create afterimages. People’s various physiological indicators are discrete and variable. However, these experiments prove that people’s visual cognitive frequency is the same, at 100 Hz, unique and unchanging.

Acknowledgements

I would like to thank Prof. Huan-Liu Hou for proofreading the manuscript, and Qian Huang for creating the images.

Ethics Declarations

The study protocol was approved by the Medical Ethics Subcommittee of the Science and Technology Ethics Committee of Nanjing University (OAP20230829001). Written informed consents were obtained from all participants. All experiments were performed in accordance with relevant guidelines and regulations. Declaration of Competing Interests
The author declares no competing interests.

Supplemental Videos

Video 1. The Illusion that High-Speed Rotating Blades Did Not Rotate (MP4)

12 white identical rectangular blades were installed on the

WT5518 Visual Characteristics Tester at 30° to each other. The flange diameter (D) was 8 cm, the blade length (L) was 11.3 cm and width (W) was 1.3 cm.

When the motor speed was set to 500 rpm, there may be a little deviation between the actual speed and the set speed. When the actual speed of the motor was equal to the set speed, 500 rpm, all participants saw the 12 fan-shaped blades fixed without rotation and the same 12 angles.

<https://pan.baidu.com/disk/main?from=homeFlow#/index?category=1>

When the actual speed of the motor was slightly higher than 500 rpm, all participants saw the 12 fan-shaped blades rotating slowly in a clockwise direction, as shown in the Video 2.

<https://pan.baidu.com/disk/main?from=homeFlow#/index?category=1>

When the actual speed of the motor was slightly below 500 rpm, all participants saw the 12 fan-shaped blades rotating slowly in an anticlockwise direction, as shown in the Video 3.

<https://pan.baidu.com/disk/main?from=homeFlow#/index?category=1>

Video 2. The Illusion that High-Speed Rotating Blades Rotate Slowly Clockwise (MP4)

12 white identical rectangular blades were installed on the WT5518 Visual Characteristics Tester at 30° to each other. The flange diameter (D) was 8 cm, the blade length (L) was 11.3 cm and width (W) was 1.3 cm.

When the motor rotated clockwise at 501 rpm, all participants saw 12 fan-shaped blades rotating slowly in a clockwise direction.

<https://pan.baidu.com/disk/main?from=homeFlow#/index?category=1>

Video 3. The Illusion that High-Speed Rotating Blades Rotate Slowly Anticlockwise (MP4)

12 white identical rectangular blades were installed on the WT5518 Visual Characteristics Tester at 30° to each other. The flange diameter (D) was 8 cm, the blade length (L) was 11.3 cm and width (W) was 1.3 cm.

When the motor rotated clockwise at 499 rpm, all participants saw 12 fan-shaped blades rotating slowly in an anticlockwise direction.

<https://pan.baidu.com/disk/main?from=homeFlow#/index?category=1>

Video 4. The Synchronous Video of Low- and High-Speed Vision (MP4)

48 white rectangular blades were installed at 7.5° to each other. The flange diameter (D) was 8 cm, the blade length (L) was 11.3 cm and width (W) was 0.4 cm.

When the motor was rotated clockwise at 125 rpm, all participants saw 48 white rectangular blades and 48 fan-shaped blades simultaneously, and they completely overlapped and fixed at 48

different angles without rotation.

<https://pan.baidu.com/disk/main?from=homeFlow#/index?category=1>

Video 5. The Illusion that Low-Speed Rotating Blades Do Not Rotate (MP4)

100 white rectangular blades were installed at 3.6° to each other. The flange diameter (D) was 13 cm, the blade length (L) was 8.8 cm and width (W) was 0.4 cm.

When the motor rotated clockwise at 60 rpm, all participants saw 100 white rectangular blades fixed at 100 different angles without rotation.

<https://pan.baidu.com/disk/main?from=homeFlow#/index?category=1>

References

1. Hubel, D. H., & Livingstone, M. S. (1987). Segregation of form, color, and stereopsis in primate area 18. *Journal of neuroscience*, 7(11), 3378-3415.
2. Livingstone, M., & Hubel, D. (1988). Segregation of form, color, movement, and depth: anatomy, physiology, and perception. *Science*, 240(4853), 740-749.
3. Al-Hashmi, A. M., Kramer, D. J., & Mullen, K. T. (2011). Human vision with a lesion of the parvocellular pathway: an optic neuritis model for selective contrast sensitivity deficits with severe loss of midget ganglion cell function. *Experimental brain research*, 215(3), 293-305.
4. Dacey, D. M., & Packer, O. S. (2003). Colour coding in the primate retina: diverse cell types and cone-specific circuitry. *Current opinion in neurobiology*, 13(4), 421-427.
5. Lee, B. B., Pokorny, J., Smith, V. C., Martin, P. R., & Valberg, A. (1990). Luminance and chromatic modulation sensitivity of macaque ganglion cells and human observers. *Journal of the Optical Society of America A*, 7(12), 2223-2236.
6. Martin, P. R., White, A. J., Goodchild, A. K., Wilder, H. D., & Sefton, A. E. (1997). Evidence that blue-on cells are part of the third geniculocortical pathway in primates. *European Journal of Neuroscience*, 9(7), 1536-1541.
7. Martin, P. R., & Solomon, S. G. (2019). The koniocellular whiteboard. *Journal of Comparative Neurology*, 527(3), 505-507.
8. Gegenfurtner, K. R. (2003). Cortical mechanisms of colour vision. *Nature Reviews Neuroscience*, 4(7), 563-572.
9. Moutoussis, K., & Zeki, S. (1997). A direct demonstration of perceptual asynchrony in vision. *Proceedings of the Royal Society of London. Series B: Biological Sciences*, 264(1380), 393-399.
10. Zeki, S. (2015). A massively asynchronous, parallel brain. *Philosophical Transactions of the Royal Society B: Biological Sciences*, 370(1668), 20140174.
11. Nassi, J. J., & Callaway, E. M. (2009). Parallel processing strategies of the primate visual system. *Nature reviews neuroscience*, 10(5), 360-372.
12. Zeki, S. (1998). REVIEW: Parallel Processing, Asynchronous Perception, and a Distributed System of Consciousness in Vision. *The Neuroscientist*, 4(5), 365-372.

-
13. American Association for Research into Nervous and Mental Diseases, Zeki, S., & Bartels, A. (1998). The autonomy of the visual systems and the modularity of conscious vision. *Philosophical Transactions of the Royal Society of London. Series B: Biological Sciences*, 353(1377), 1911-1914.
 14. Anssari, N., Vosoughi, R., Mullen, K., & Mansouri, B. (2020). Selective colour vision deficits in multiple sclerosis at different temporal stages. *Neuro-ophthalmology*, 44(1), 16-23.
 15. Cantó-Cerdán, M., Cacho-Martínez, P., & García-Muñoz, Á. (2020). Delphi methodology for symptomatology associated with visual dysfunctions. *Scientific Reports*, 10(1), 19403.
 16. Moura, A. L. D. A., Teixeira, R. A. A., Oiwa, N. N., Costa, M. F., Feitosa-Santana, C., Callegaro, D., ... & Ventura, D. F. (2008). Chromatic discrimination losses in multiple sclerosis patients with and without optic neuritis using the Cambridge Colour Test. *Visual Neuroscience*, 25(3), 463-468.
 17. Fu, Y., Yan, W., Shen, M., & Chen, H. (2021). Does consciousness overflow cognitive access? Novel insights from the new phenomenon of attribute amnesia. *Science China Life Sciences*, 64(6), 847-860.
 18. Zeki, S., & Ffytche, D. H. (1998). The Riddoch syndrome: insights into the neurobiology of conscious vision. *Brain: a journal of neurology*, 121(1), 25-45.
 19. Wu, S., Wang, M., & Zou, Y. (2018). Bidirectional cognitive computing method supported by cloud technology. *Cognitive Systems Research*, 52, 615-621.
 20. Davis, T., & Goldwater, M. (2021). Using model-based neuroimaging to adjudicate structured and continuous representational accounts in same-different categorization and beyond. *Current Opinion in Behavioral Sciences*, 37, 103-108.
 21. Forbus, K. D., & Lovett, A. (2021). Same/different in visual reasoning. *Current Opinion in Behavioral Sciences*, 37, 63-68.
 22. Fang, F., & Hu, H. (2021). Recent progress on mechanisms of human cognition and brain disorders. *Science China Life Sciences*, 64(6), 843-846.

Copyright: ©2025 Laiyou Huang. This is an open-access article distributed under the terms of the Creative Commons Attribution License, which permits unrestricted use, distribution, and reproduction in any medium, provided the original author and source are credited.